ELSEVIER

Journal of Biomechanics 38 (2005) 1441–1449

JOURNAL OF BIOMECHANICS

www.elsevier.com/locate/jbiomech
www.JBiomech.com

Viscoelastic response of the finger pad to incremental tangential displacements

Todd C. Pataky*, Mark L. Latash, Vladimir M. Zatsiorsky

Department of Kinesiology, The Pennsylvania State University, USA

Accepted 7 July 2004

Abstract

The finger pads of eight subjects were loaded by tangential displacement (x—perpendicular to the long axis of the finger) of a contacted surface when the distal and proximal interphalangeal joints (DIP and PIP, respectively) were alternately constrained. The finger pad responded in a linearly viscoelastic manner during loading, but exhibited highly nonlinear behavior upon unloading. The observed tangential force (F_T) relaxations were nonlinear and could be modeled well by a logarithmic function. The average F_T relaxation duration (τ) was 11.8 s. Apparent tangential stiffness (k_T), determined by F_T after relaxation, varied linearly with normal force. With the DIP joints constrained the fingers showed significantly larger stiffness than with the PIP joints constrained ($p<0.001$). Implications for finger force coordination studies are discussed.

Keywords: Finger pad; Viscoelasticity; Stiffness; Material properties; Fingers

1. Introduction

The finger pads constitute the mechanical interface between human and grasped object. Since dexterous manipulation requires highly precise spatial and temporal control of contact forces, knowledge of the mechanical properties of the finger pads may be important for understanding finger coordination.

The finger pads experience large deformation under even small loads. Normal deformation of 2 mm has been reported for loads as low as 1 N (Serina et al., 1997), and tangential deformation of 3.5 mm has been reported for tangential loads and contact forces of approximately 2 N (Nakazawa et al., 2000). Of importance to coordination studies, highly compliant soft tissue affects the moment arm of a contact force with respect to a grasped object. Additionally, it is conceivable that localized strain fields might be the source of objective optimization functions (e.g. minimizing local strain energy) that could be used by the central nervous system (CNS) for coordinating finger forces; it has been speculated that pinch force under tangential load is modulated by the finger pad mechanical properties (Jones and Hunter, 1992). The large number of strain-sensitive mechanoreceptors and their large representation in the sensorimotor cortex (Johansson et al., 1980; Gardner, 1988) supports the possibility for strain-based optimization. The possibility is intuitively supported by experimental evidence for perception: certain external mechanical variables relevant to grasping such as tangential force (Paré et al., 2002) and friction coefficients (Smith et al., 2002) are perceived accurately by some individuals.

Viscoelasticity might also affect how finger forces are coordinated. Finger pad viscoelasticity implies that a force controller must also consider tissue creep, and that a position controller must also consider relaxation. In other words, controlling the bone does not control the pad-object interface unless viscoelastic phenomena are

*Corresponding author. Biomechanics Laboratory, 39 Recreation Building, University Park, PA 16802, USA. Tel.: +1-814-865-3445; fax: +1-814-865-2441.

E-mail address: tcp120@psu.edu (T.C. Pataky).

0021-9290/$ - see front matter © 2004 Elsevier Ltd. All rights reserved.
doi:10.1016/j.jbiomech.2004.07.004

incorporated in the control scheme. Stress relaxation of the human heel pad at a constant 40% strain was found to be approximately 75% after 1 min (Miller-Young et al., 2002). Relaxation of this magnitude, if similar for the finger pad, would surely affect grasping dynamics. While uniaxial viscoelastic behavior has been demonstrated both for isolated human skin (Pan et al., 1998), and for the finger pad under normal compression (e.g. Srinivasan et al., 1992; Serina et al., 1997; Pawluk and Howe, 1999; Jindrich et al., 2003), no study has examined viscoelastic relaxation of the finger pad when loaded tangentially.

Since total finger deformation results also from distal interphalangeal (DIP) and proximal interphalangeal (PIP) joint compliance, the present study tested, respectively: (a) viscoelastic relaxation of the finger pad subjected to tangential displacement load and (b) contribution of the DIP joints to the lumped finger compliance. Given the nonlinear geometry and lumped material response, the present purpose was not to model the finger pad in a constitutive sense, but rather in a phenomenological sense (similar to the Nakazawa et al. 2000 study). An incremental loading protocol was adopted—a protocol which can be used to characterize quasi-linear viscoelastic materials (Sarver et al., 2003). In short, the present study extends the work of Nakazawa et al. (2000) to examine viscoleastic response and DIP compliance.

2. Methods

2.1. Subjects

Nine subjects volunteered to participate in the study (Table 1). All subjects were right-handed; only right hands were tested. All denied history of upper limb pathology. Prior to participation all subjects gave informed consent according to the policies of the Office for Research Protections of the Pennsylvania State University.

Table 1
Subject information

	N	Age (years)	Height (cm)	Body mass (kg)	Hand length (cm)
Protocol V	3♂	28.0 (2.0)	177.7 (4.0)	72.7 (4.0)	18.6 (0.9)
Protocol DIP	3♂	25.7 (0.6)	182.0 (7.9)	74.2 (5.8)	18.3 (0.7)
	3♀	24.3 (2.1)	165.1 (2.5)	60.6 (4.8)	16.7 (0.4)

N is the number of subjects. Standard deviations appear in parentheses. Refer to Section 2.3 for a description of the protocols.

2.2. Apparatus

An aluminum finger vise was constructed to immobilize a subject's finger while allowing for finger pad compression against a force transducer that could be displaced tangentially with respect to the finger (Fig. 1). The subject's finger was placed in the horizontal plane on an aluminum platform and was clamped mediolaterally at either the DIP or PIP with two cylindrical vise faces (diameter: 2.3 cm). The cylinder clamps could be positioned anywhere along the longitudinal axis of the finger via two sliders attached to the platform.

The surface of a three-dimensional force transducer (model: Nano-17; ATI Industrial Automation, Garner, NC, USA; accuracy = 0.04 N) was attached to an aluminum base and was placed level with the finger platform. The raw force transducer voltages were routed to a 12-bit analog-digital converter (PCI-6031, National Instruments, Austin, TX, USA) and sampled at 50 Hz using LabView (National Instruments). To prevent finger slipping 100-grit sandpaper (Carborundum Abrasives, North America) was attached to the surface of the transducer using Superbonder silicone adhesive (FPC Corporation, Wauconda, IL). The coefficient of static friction (μ_s) between the finger pad and the sandpaper was measured to be approximately 1.4 (previously measured: Zatsiorsky et al., 2003).

The subject's finger was placed in the experimental apparatus such that the transducer center was coincident with the apex of the finger pad and such that the finger's longitudinal axis was parallel to the long axis of the apparatus. The cylinder clamps were positioned at the center of either the DIP or PIP and were then tightened with a screwdriver to the maximum tightness

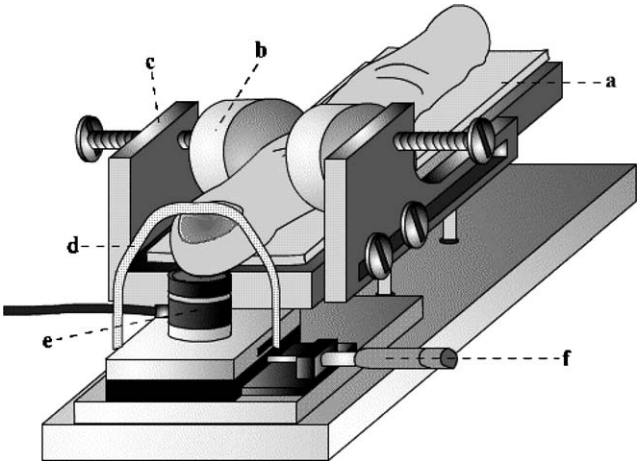

Fig. 1. Experimental apparatus. The subjects' fingers were placed individually on an aluminum platform (a) and were held in place by cylindrical aluminum clamps (b) that could be positioned at different places along the finger's longitudinal axis by sliders (c). An elastic band (d) was used to compress the finger against a sandpaper-surfaced force transducer (e). The transducer was then displaced tangentially with respect to the finger via a micrometer positioning slide (f).

tolerable to the subject. The subjects were found to tolerate the tightness quite well, and for all subjects the cylinders could be tightened until displacement of the superficial skin surrounding the DIP joint made further tightening impossible (i.e. the displaced skin prevented cylinder turning). The compressive forces of the cylinder clamps on the subjects' DIP joints were not quantified.

Finger compression against the surface of the force transducer was achieved by elastic bands that were fed through a hole in the aluminum base to which the transducer was attached (the possibility that the elastic band contributed to the measured forces was discounted; see Section 3.1). The bands were looped around the proximal edge of the fingernail. Three different elastic bands were used to achieve normal force (F_N) levels of approximately 1, 3, and 5 N, respectively. The actual F_N varied with the size of the finger and the tangential displacement of the transducer (due to changes in band length) and was measured to be in the range: [0.4, 7.8 N].

The force transducer was displaced in the mediolateral direction via a micrometer positioning slide (model: H14D88-101Y; Techno Inc., New Hyde Park, NJ, USA) to which the transducer's aluminum base was attached. The micrometer positioning slide had a manufacturer specified accuracy of 0.0025 mm. With the elastic band in place, the micrometer positioning slide was adjusted finely such that the magnitude of the registered F_T was less than 0.1 N. When this criterion baseline F_T was met, the experimenter triggered data collection, and the trial commenced.

2.3. Procedure

2.3.1. Pre-experiment

Subjects were required to wash their hands before testing began in order to keep μ_s as constant as possible across subjects. Fresh sandpaper was glued to the transducer at the beginning of each subject's testing session to avoid confounding effects of sandpaper wear. To prevent boredom-induced finger movements, subjects were instructed to relax their arm and pay attention only to a DVD film that they selected prior to testing.

2.3.2. Loading protocol

The transducer was displaced tangentially in either the medial (Med) or lateral (Lat) direction (see Table 2 for direction definitions) in 0.635 mm increments with 10 s pauses at each increment. All subjects had all four fingers tested: index (I), middle (M), ring (R), and little (L). Since the experimenter applied the displacements manually using the micrometer positioning slide's dial, the ramp-like tangential loadings were not precisely controlled—the new increment was achieved within 1 s and thus the average loading velocity was approximately 0.635 mm s^{-1}. No analyses of the loading interval were made. Loading was terminated either after eight increments or when F_T exceeded F_N, which ever came first. The latter trial termination criterion prevented the potentially confounding effects of slipping. Unloading then followed in decrements of 0.318 mm (half of the loading increment) until the registered F_T reached zero. Due to relaxation, the number of unloading decrements was less than twice the number of loading increments. The total trial duration was between 120 and 200 s.

Table 2
Experimental conditions

Protocol	Factor	Levels
V, DIP	Finger	I, M, R, L
V, DIP	Normal force	~1, 3, 5 N
V, DIP	Load direction	Med, Lat
V	Load/unload	L, UL
DIP	Joint	DIP, PIP (I and M only)
DIP	Gender	♀, ♂

All subjects had all four fingers tested (index, middle, ring, and little; I, M, R, and L, respectively). The medial (Med) LOAD DIRECTION was defined as tissue displacement toward the thumb (i.e. left from the subject's point of view), and lateral (Lat) loading was away from the thumb. Three levels of NORMAL FORCE were applied (see Section 2). Protocol V examined viscoelasticity and Protocol DIP examined DIP compliance. Females were tested for only Protocol DIP; unloading was not included in Protocol DIP.

2.3.3. Experimental conditions

Six experimental conditions were tested (Table 2). Because pilot studies were lengthy, the conditions were divided between two protocols: Protocol V examined viscoelasticty and Protocol DIP examined the contribution of DIP compliance to the endpoint lumped response. Despite the inclusion of only three subjects in Protocol V (Table 2), the only data peculiar to $N=3$ were unloading relaxation and hysteresis data (see Section 2.4).

The experimental conditions were changed according to the following hierarchy: FINGER, JOINT, NORMAL FORCE, LOAD DIRECTION. That is, trials for both load directions were conducted before changing F_N, and all three F_N levels were applied before changing the joint, etc. This non-random order of experimental condition presentation was not considered to confound the data because subjects were not actively involved in an experimental task. In the interest of subject time, only the I and M fingers were tested under Protocol DIP. The force transducers were software zeroed after each change of finger (no drift was observed).

2.4. Data processing and statistics

All data were processed using Matlab software (The MathWorks Inc., Natick, MA, USA). Statistics were calculated using both Matlab and Minitab software

(Minitab Inc., State College, PA, USA). All statistical analyses were performed at a significance level $\alpha = 0.05$.

The force data were truncated into the individual relaxation intervals (the ease of such truncation is illustrated in Fig. 2). After truncation, the absolute value of the raw F_T signal was zero-phase forward-and-reverse-filtered using a second-order low-pass Butterworth filter with a cutoff frequency of 10 Hz. Subsequent data processing occurred in three stages: relaxation, stiffness, and hysteresis. Each stage was reliant on the results of the previous stage.

2.4.1. Relaxation

The F_T relaxation was modeled phenomenologically as a logarithmic change in the rate of F_T relaxation (dF_T/dt):

$$dF_T/dt = \alpha_1 \ln(t) + \alpha_2. \quad (1)$$

This accurately; simpler linear exponential decay models were not as particular model was found to model the data most successful at reproducing pilot data. The relaxation was not modeled as has been done for soft biological tissues in the past (e.g. Fung, 1993) because of the complex viscoelastic deformation; such modeling would be misleading because the current data set should not be used for constitutive modeling (the present data could only be used in a constitutive sense only through validation of a finite element model or inverse finite element analysis). The tissue was assumed to be completely relaxed for $dF_T/dt = 0$. For isolated skin, Pan et al. (1998) found that complete relaxation took more than 1000 s. Unsurprisingly the 10 s intervals of relaxation of the current study were found to be insufficient to observe complete tissue relaxation.

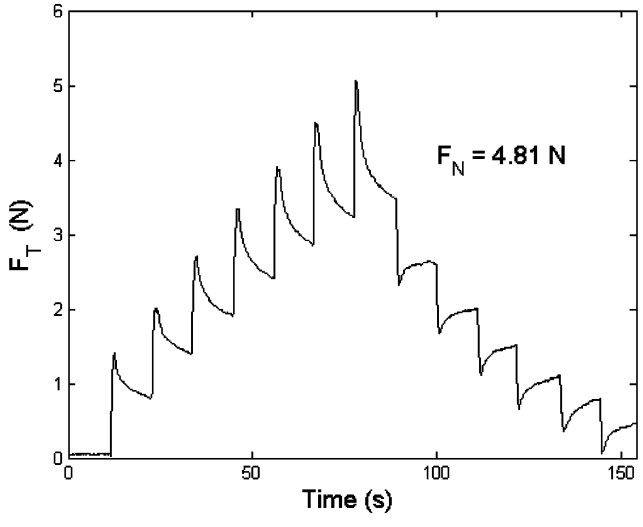

Fig. 2. Raw F_T data for a trial with average $F_N = 4.81$ N. The unloading increments commenced at approximately 80 s in the trial shown. The beginning of the relaxation interval was chosen by eye from the first point of continuous F_T decrease and the end was chosen by eye at the first point of the steep F_T rise.

The calculated dF_T/dt was filtered (with the same filter that was used for the raw F_T signal—see Section 2.4), and linear regression was applied to the time-differentiated F_T data according to Eq. (1). This linear regression was justified by the data of that Pan et al. (1998) for skin relaxation. However, due to the logarithmic nature of Eq. (1), the first second of the filtered dF_T/dt was quite erratic and thus only the $dF_T(t)/dt$ signal for $t > 1$ s was used in the regression.

Relaxation was modeled using the above technique for both loading and unloading. However, since unloading relaxation actually involves increasing force (as is expected from viscoelastic theory), the unloading data were 'rectified' such that the initial F_T value before relaxation was greater than the $(F_T)_{sat}$. This rectification was achieved by subtracting all F_T values on a given relaxation interval by $(F_T)_{sat}$, and then considering the absolute value of the signal. The correlation coefficient (r) between the fitted and the actual F_T signal was used as an estimate of the appropriateness of fit.

In addition to assessing the appropriateness of the fits, the values of the fitted parameters (α_i) and the calculated τ values were independently compared across experimental conditions. This was done using separate ANOVAs for each parameter. As the α_i parameters were found to depend on the normal force, the α_i parameters for all subjects were linearly regressed on F_N.

2.4.2. Stiffness

The elastic behavior of soft tissues is typically determined based on the total deformation rate and the inelastic strain rate (Rubin and Bodner, 2002). Since the required rates were neither measured nor controlled, and since strain was not quantified, an atypical rate-independent elasticity measure was required.

A 'saturation' force $(F_T)_{sat}$ [$(F_T)_{sat} = F_T$ for $dF_T/dt = 0$] was calculated as follows: firstly, the time to relaxation (τ) was calculated as

$$dF_T(\tau)/dt = 0 \quad (2)$$

which implies:

$$\tau = e^{-\alpha_2/\alpha_1} \quad (3)$$

and thus

$$(F_T)_{sat} = \alpha_1 \tau(\ln \tau - 1) + \alpha_2 \tau + F_T(t = t_0) \quad (4)$$

by the integration of Eq. (1). Let us now define 'apparent tangential stiffness' (k_T) as the relation between $(F_T)_{sat}$ and the applied displacement load (x) for a given F_N magnitude. A loading (L) curve [$(F_T)_L$] and an unloading (UL) curve [$(F_T)_{UL}$] were characterized separately. The loading curve was approximated by linear first-order polynomial regression. The $(k_T)_{UL}$ curve was found (by simple trial-and-error curve fitting) to best be approximated by the function:

$$(F_T)_{UL} = \lambda_1 + \lambda_2 e^x + \lambda_3 x e^x, \quad (5)$$

It was assumed that the points: $F_T(x=0)=0$ and $F_T(x=x_{max})$ lay on both the loading and unloading curves, where x_{max} was the maximum displacement increment achieved. Similar to the (α_i, β_i) comparisons, the parameters characterizing $(k_T)_L$ and $(k_T)_{UL}$ distributions (slope and λ_i, respectively) were compared across different experimental conditions using ANOVA.

2.4.3. Hysteresis

Hysteresis was calculated analytically as the area between the fitted $(k_T)_L$ and $(k_T)_{UL}$ curves for the displacement interval: $(<x<x_{max})$ and was denoted: A_{hyst}. Since $(k_T)_L$ and $(k_T)_{UL}$ represent the long-term behavior of the finger pad, 'hysteresis', as used here, has a meaning distinct from typical cyclical loading tests of materials. Note that for a linearly viscoelastic material, the Boltzmann superposition principle applies (Lakes, 1999). Thus, if the finger pad aggregately behaves in a linearly viscoelastic manner, the measured A_{hyst} would be zero because the applied x would uniquely determine the $(F_T)_{sat}$ independent of loading/unloading. After calculating the A_{hyst}, energy loss due to unloading was compared across experimental conditions using ANOVA. One-sided t-tests were used to compare A_{hyst} between fingers.

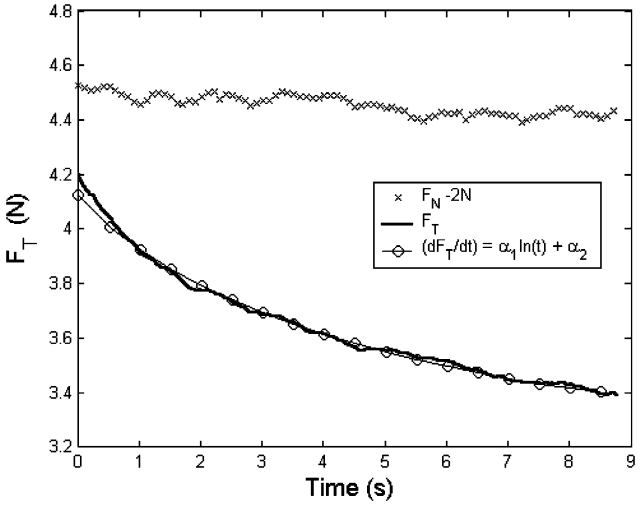

Fig. 3. Example of F_T relaxation: the F_N shown is the actual F_N signal which is less than 2 N (for compactness of the figure). The illustrated trial had relaxation time $\tau = 13.9$ s and saturation force $(F_T)_{sat} = 3.12$ N. The r^2 value for the fitted data was 0.993.

3. Results

3.1. Relaxation

All F_T relaxations exhibited nonlinear behavior. An example relaxation interval for $F_N = 4.9$ N is shown in Fig. 3. The F_T tended to decrease relatively rapidly over the first 3–4 s, and then the rate of relaxation gradually decreased until F_T saturated after an average interval of $\tau = 11.2 \pm 3.2$ s. ANOVA found no significant differences in τ between fingers ($p = 0.1$). The possibility that the elastic band used to compress the finger pad against the transducer contributed to the observed relaxation was discounted because F_N was not observed to relax; linear regressions of F_N over the trial time revealed an average slope of 0.0042 N/s (considering only slope magnitude). The same linear regression applied to F_T found an average slope of 0.039 N/s, which was nearly nine times greater than the slope of the F_N. Since the elastic band acted predominantly in the normal direction, it was concluded that the observed relaxation was not due to viscoelastic effects of the elastic band. The possibility that the moment caused by differing tension in the two sides of the elastic band contributed to the relaxation was also discounted. Based on apparatus geometry, the tension difference between the two sides of the elastic band was, for the maximum F_N and the maximum x, on the order of 0.05 N. This is two orders of magnitude smaller than the recorded F_T. The possibility that slip led to the observed relaxation was also considered improbable because $F_T < F_N$ and μ_s was certainly greater than 1.0.

The relaxation parameters are presented for each finger and joint constraint as slopes and intercepts of linear regressions on F_N (Table 3). For example, for $F_N = 1$ N, the average relaxation parameters for the I finger with the DIP constraint were: $\alpha_1 = 0.0377$ and

Table 3
Slopes (m), y-intercepts (y_0), and correlation coefficients (r) of linear regressions of the relaxation parameters on normal force across all subjects

Finger	Joint	α_1			α_2		
		M	y_0	r	M	y_0	r
I	DIP	0.0075	0.0302	0.43	−0.0183	−0.0664	0.48
	PIP	0.0033	0.0189	0.38	−0.0085	−0.0425	0.45
M	DIP	0.0060	0.0271	0.33	−0.0151	−0.0577	0.52
	PIP	0.0028	0.0179	0.30	−0.0063	−0.0428	0.32
R	DIP	0.0056	0.0187	0.43	−0.0133	−0.0420	0.50
L	DIP	0.0079	0.0141	0.54	−0.0190	−0.0310	0.60

The DIP and PIP data were based on the data of eight subjects and three subjects, respectively. The average r value of the α_i regressions was 0.45.

Table 4
P-values from ANOVA of the relaxation parameters

Factor	τ	α_1	α_2
Gender	<0.001	<0.001	0.018
Subject	<0.001	<0.001	<0.001
Finger	0.049	<0.001	<0.001
Joint	0.007	<0.001	<0.001
Normal force	**0.438**	<0.001	<0.001
Load direction	**0.708**	0.237	0.488
Load/unload	**0.101**	<0.001	<0.001
Displacement	<0.001	<0.001	<0.001

P-values that failed to reach significance are highlighted in bold.

$\alpha_2 = -0.0847$. The fits of the regressions, however, were generally poor: an average r value of only 0.45 was found. We nevertheless felt that reporting the regression coefficients would be useful to the readership. ANOVA found significant effects of most of the experimental factors on the parameters. The p-values from the ANOVAs are presented in Table 4. Even though significant differences were found between loading and unloading, the data presented in Table 3 are for loading only because of the small number of subjects tested for unloading. In general, the magnitude of the relaxation parameters decreased during unloading by close to 50%.

Fig. 3 shows that Eq. (1) reproduced the F_T relaxation quite well. Importantly, the predicted F_T regularly saturated below the measured F_T at the end of the relaxation interval (as can be seen in Fig. 3). The magnitude of the F_T relaxation may be expressed as a percentage of the initial force $F_T(t=0)$. For the index finger with DIP constrained, $\tau = 10.8$, $F_N = 1$ N, and $F_T(t=0) = 1$ N, Eq. (1) predicts the average F_T relaxation to be 35.3%.

3.2. Stiffness

Long-term elasticity, as described in Section 2.4.2, was represented by the stiffness k_T. The k_T values were found to vary linearly with F_N. Fig. 4 illustrates the linear regression of k_T on F_N for the index finger. All subjects tended to show a linear k_T relation with F_N, but individuals showed noticeable differences from the average curve. The k_T regression was not forced through the origin because it is unknown whether the relation remains linear for small F_N. The average slopes and intercepts for the k_T regression are presented in Table 5. With the DIP joints constrained, the fingers showed significantly larger stiffness than with the PIP joints constrained ($p<0.001$).

3.3. Hysteresis

All trials produced hysteresis (as defined in Section 2.4.3) with substantial energy loss (average: 41.3%)

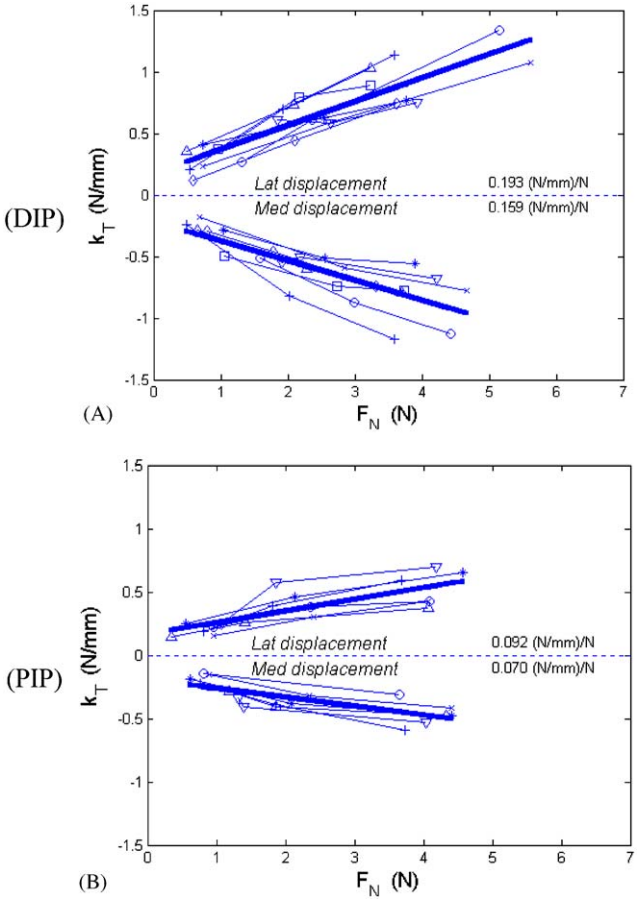

Fig. 4. Tangential finger pad stiffness (k_T) as a function of normal force for the index finger with the distal interphalangeal joint (A) and proximal interphalangeal joint (B) constrained. Positive and negative k_T indicate lateral (Lat) and medial (Med) tissue displacement, respectively. Different symbols correspond to different subjects, and the thick solid line is the linear regression over all subjects.

implying nonlinear viscoelastic behavior. A typical hysteresis curve is presented in Fig. 5. This figure shows that Eq. (3) fit the $(k_T)_{UL}$ curve very well, which was also true of most trials; the median r^2 value across all $(k_T)_{UL}$ fits was 0.996. ANOVA found no significant effects of SUBJECT, NORMAL FORCE, or LOAD DIRECTION on A_{hyst} ($p=0.393$, 0.375, and 0.877, respectively) but did find significant effects of FINGER and x_{max} ($p=0.008$ and 0.005, respectively). The differences between fingers were not large (see Fig. 6), and one-sided t-tests revealed significant differences between only the I–R and I–L pairs. The A_{hyst} increased approximately linearly with x_{max} (not shown), and varied from approximately 32% (from a minimum x_{max} of 2.5 mm), to approximately 47% (to a maximum x_{max} of 5.7 mm).

4. Discussion

This is the first study to report the viscoelastic relaxation response of the finger pad subject to shear

Table 5
Tangential finger pad stiffness (k_T) as a function of normal force (F_N)

Finger	Joint	Med			Lat		
		m	y_0	r	m	y_0	r
I	DIP	0.160	0.213	0.81	0.193	0.175	0.89
	PIP	0.071	0.192	0.79	0.093	0.162	0.79
M	DIP	0.101	0.235	0.81	0.133	0.170	0.79
	PIP	0.057	0.207	0.73	0.053	0.206	0.41
R	DIP	0.107	0.166	0.82	0.131	0.193	0.86
L	DIP	0.119	0.193	0.80	0.153	0.191	0.81

The slopes (m) have units: mm^{-1} and the y-intercepts (y_0) have units: $N\,mm^{-1}$ and were determined by linear regression of k_T on F_N for all subjects (e.g. for $F_N = 1$ N, the average k_T for medial displacement was $0.373\,N\,mm^{-1}$). The regressions' correlation coefficients (r) are also listed. The values are presented for the medial (Med) and lateral (Lat) directions separately. The DIP and PIP data were based on the data of eight subjects and three subjects, respectively.

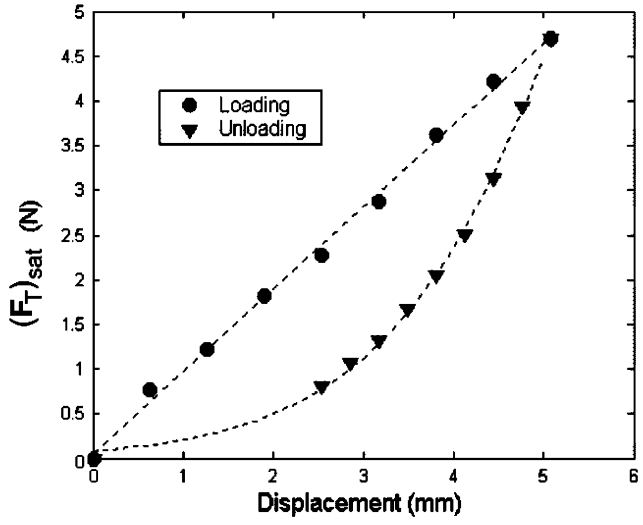

Fig. 5. Loading and unloading tangential saturation force response: a representative example. This trial was performed on the ring finger with the distal interphalangeal joint constrained and with a normal force of 5.7 N. The trial shown had the following parameters: loading stiffness $k_T = 0.92\,N\,mm^{-1}$, $\lambda = [-0.017, 0.097, -0.013]$, and hysteresis $A_{hyst} = 45.3\%$. The loading and unloading curves had r^2 values of 0.997 and 0.999, respectively.

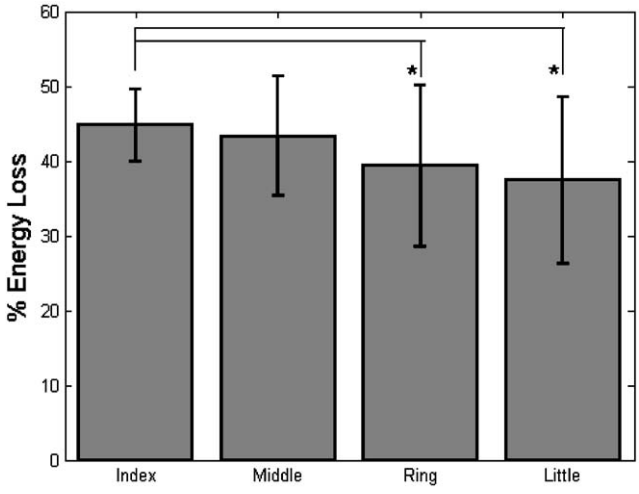

Fig. 6. Percentage energy loss due to unloading the fingers. The index finger experienced significantly more energy loss than the ring and little fingers (indicated by asterisks; $p = 0.035$ and 0.014, respectively). The difference between the middle and ring fingers was marginally significant ($p = 0.052$).

load. Incremental loading induced behavior consistent with linearly viscoelasticity (i.e. a linear F_T/x relation for constant time; in this case $t = \infty$), but large hysteresis upon unloading is indicative of nonlinear viscoelastic behavior. The F_T relaxation was quite large (on the order of tens of percents of the initial force) over a relatively short period of time (˜10 s).

Pan et al. (1998) found relaxation times for isolated skin on the order of 1000 s. The discrepancy of these results and our findings is probably due to the role of subcutaneous structures in the intact finger pad as compared to isolated skin. In particular, skin strains under the current loading protocol may have been negligible compared to subcutaneous tissue strains.

While uniaxial finger pad viscoelasticity (under normal load) has been addressed previously (e.g. Jindrich et al., 2003; Pawluk et al., 1999), this is the first to investigate viscoelasticity under shear load. Since this was no uniaxial test, it is not immediately feasible to compare experimental values. Our data could be compared to the constitutive model parameters of the previous studies using inverse finite element analysis (FEA), but such analysis is beyond the scope of the paper. A comparison of the current k_T data with published data is contrastingly immediately feasible. For example, $(k_T)_M$ with $F_N = 1.9$ N was reported to be approximately 0.45 and $0.43\,N\,mm^{-1}$ by Nakazawa et al. (2000) and the current study, respectively. The Nakazawa et al. study, like the current study, also showed an approximately constant k_T with increased F_T.

There were, however, two major discrepancies between the data of Nakazawa et al. (2000) and the present data: the Nakazawa et al. study found neither direction dependence nor viscoelastic creep (they held F_T constant rather than x). The null directional dependence may have been due to unique subjects (they only tested three), or to low statistical power. The presently observed direction dependence of k_T may help to explain previous results that finger coordination patterns depend on load direction (Jones and Hunter, 1992). An explanation for the lack of viscoelastic response in the Nakazawa et al. study is more elusive, especially since their deformation rate ($\tilde{}20\,N\,s^{-1}$) was much greater than that used in the present study. The discrepancies in the two studies may also be due to the frictional conditions in the Nakazawa study (which were not described) and the fact that they measured the displacement and reaction forces of the platform on which the finger was resting rather than at the finger–platform interface itself.

Previous research on finger pad viscoelasticity employed exponential relaxation models (e.g. Fung, 1993; Pawluk and Howe, 1999; Jindrich et al., 2003); exponential models less accurately modeled our data than the employed logarithmic equation. We believe that there may be two sources of discrepancy between our data and those data previously modeled: (1) complex deformation and (2) equation complexity. Our experimental protocol involved complex (i.e. neither axisymmetric nor uniaxial) loading with large normal and shear components. Thus simple constitutive relations could not be derived. The cited studies derived the constitutive relations assuming uniaxial loading. The equations used by others included, for example, the much more complex Prony series modeling (Miller-Young et al., 2002). Since Prony series equations incorporate many coefficients, interpretation of the coefficients can be difficult.

Perhaps the most surprising result of the present study was the large amount of hysteresis. This finding might be attributable to blood occlusion caused by increasing pressure in the soft finger pad tissue. Alternatively, the hysteresis may have been an after-effect of finger pad substructure shifting rather than representing an amalgamation of various viscoelastic substances. The possibility that the hysteresis was due to finger slipping was considered unlikely, not only because $F_T < F_N$, but also because if slight slipping did occur, such a dramatic hysteresis curve would not be produced if the finger pad behaved in a linearly viscoelastic manner en masse. If the finger pad actually does behave linearly viscoelastically, then another explanation for the large hysteresis is that the employed F_T relaxation interval (Δt) was insufficient to accurately estimate $(F_T)_{sat}$. In other words, the $(k_T)_L$ and $(k_T)_{UL}$ curves could be skewed apart by overestimation and underestimation of $[(F_T)_{sat}]_L$ and $[(F_T)_{sat}]_{UL}$, respectively. This possibility could be addressed by testing the sensitivity of a viscoelastic model to $\Delta t < \tau$, but pilot studies with Δt of over 1 min suggested that $\Delta t < \tau$ did not contribute to the observed hysteresis.

It was observed (Protocol DIP) that joint compliance in the DIP cannot be neglected in favor of the isolated finger pad when considering the k_T of the finger system. The observed DIP compliance suggests that the PIP compliance might also significantly contribute to k_T, but this was not measured here. Studies of finger force coordination that attempt to employ finger stiffness data should consider all factors contributing to k_T when quantifying finger compliance. Additionally, finger force coordination studies should consider what performance variables are preferentially stabilized by the nervous system: if force is stabilized, then creep along the tangential axis can affect the moment arm of normal forces, and if bone position is stabilized, then relaxation will affect the total force imparted on the grasped object.

The present data, while derived from aggregate materials testing, may be useful for studies of finger force production and coordination, for FEA or constitutive modeling, or for robotic manipulator studies. The authors intend to investigate whether using uniaxial data from isolated skin (Pan et al., 1998) that has been used previously for FEA by Wu et al. (2002) can reproduce the results herein observed.

References

Fung, Y., 1993. Bioviscoelastic solids. In: Biomechanics: Mechanical Properties of Living Tissues, Springer, New York, pp. 242-320.

Gardner, E.P., 1988. Somatosensory cortical mechanisms of feature detection in tactile and kinesthetic discrimination. Canadian Journal of Physiology and Pharmacology 66, 439–454.

Jindrich, D.L., Zhou, Y., Becker, T., Dennerlein, J.T., 2003. Nonlinear viscoelastic models predict fingertip pulp force- displacement characteristics during voluntary tapping. Journal of Biomechanics 36, 497–503.

Johansson, R.S., Vallbo, A.B., Westling, G., 1980. Thresholds of mechanosensitive afferents in the human hand as measured with von Frey hairs. Brain Research 184, 343–351.

Jones, L.A., Hunter, I.W., 1992. Changes in pinch force with bidirectional load forces. Journal of Motor Behavior 24 (2), 157–164.

Lakes, R.S., 1999. Viscoelastic Solids. CRC Press, New York.

Miller-Young, J.E., Duncan, N.A., Baroud, G., 2002. Material properties of the human calcaneal fat pad in compression: experiment and theory. Journal of Biomechanics 35, 1523–1531.

Nakazawa, N., Ikeura, R., Inooka, H., 2000. Characteristics of human fingertips in the shearing direction. Biological Cybernetics 82, 207–214.

Pan, L., Zan, L., Foster, F.S., 1998. Ultrasonic and viscoelastic properties of skin under transverse mechanical stress in vitro. Ultrasound in Medicine and Biology 24, 995–1007.

Paré, M., Carnahan, H., Smith, A.M., 2002. Magnitude estimation of tangential force applied to the fingerpad. Experimental in Brain Research 142, 342–348.

Pawluk, D.T., Howe, R.D., 1999. Dynamic contact of the human fingerpad against a flat surface. Journal of Biomechanical Engineering 121 (6), 605–611.

Rubin, M.B., Bodner, S.R., 2002. A three-dimensional nonlinear model for dissipative response of soft tissue. International Journal of Solids and Structures 39, 5081–5099.

Sarver, J.J., Robinson, P.S., Elliott, D.M., 2003. Methods for quasi-linear viscoelastic modeling of soft tissue: application to incremental stress-relaxation experiments. Journal of Biomechanical Engineering, Transactions of the ASME 125, 754–759.

Serina, E.R., Mote Jr., C.D., Rempel, D., 1997. Force response of the fingertip pulp to repeated compression—effects of loading rate, loading angle and anthropometry. Journal of Biomechanics 30, 1035–1040.

Smith, A.M., Chapman, C.E., Deslandes, M., Langlais, J.S., Thibodeau, M.P., 2002. Role of friction and tangential force variation in the subjective scaling of tactile roughness. Experimental Brain Research 144, 211–223.

Srinivasan, M.A., Gulati, R.J., Dandekar, K., 1992. In vivo compressibility of the human fingertip. In: Bidez, M.W. (Ed.), Advances in Bioengineering, Proceedings of the ASME, vol. 22, pp. 573–576.

Wu, J.Z., Dong, R.G., Rakheja, S., Schopper, A.W., 2002. Simulation of mechanical responses of fingertip to dynamic loading. Medical Engineering & Physics 24, 253–264.

Zatsiorsky, V.M., Gao, F., Latash, M.L., 2003. Prehension synergies: effects of object geometry and prescribed torques. Experimental Brain Research 148 (1), 77–87.